

---

# NPMixer: Hierarchical Neighboring Patch Mixing for Time Series Forecasting

---

Jung Min Choi<sup>1</sup> Vijaya Krishna Yalavarthi<sup>1</sup> Lars Schmidt-Thieme<sup>1</sup>

## Abstract

Multivariate time series forecasting remains a challenge due to the complexity of local temporal dynamics and global dependencies across multiple variables. In this paper, we propose **Neighboring Patching Mixer (NPMixer)**, a hierarchical architecture featuring a Learnable Stationary Wavelet Transform that adaptively learns filter coefficients to decompose signals into trend and detail components in a data-dependent manner. Our framework introduces a Neighboring Mixer Block that captures local temporal dynamics through a series of hierarchical MLP layers operating on non-overlapping patches. Specifically, the mixer block utilizes MLPs to learn temporal patterns within and across these patches, expanding the receptive field to capture multi-scale dependencies. A Channel-Mixing Encoder is applied to high-frequency components to learn channel correlations while preserving the stability of the underlying global trend. Extensive experiments on seven benchmark datasets demonstrate that NPMixer consistently outperforms state-of-the-art models, achieving better performance in 20 out of 28 (71.4%) evaluated experimental setups for MSE.

## 1. Introduction

Time series forecasting (TSF) is utilized across an extensive range of domains, including climate science (Max Planck Institute for Biogeochemistry, 2024), electricity consumption (Trindade, 2015), and traffic analysis (California Department of Transportation (Caltrans), 2024), among various other research areas. Recently, to achieve more precise forecasting performance, a significant volume of research has explored deep learning architectures, moving beyond traditional statistical methods such as ARIMA (Box et al.,

2015). Transformer (Vaswani et al., 2017)-based models, such as Informer (Zhou et al., 2021), FEDformer (Zhou et al., 2022), and Crossformer (Zhang & Yan, 2023), have proven effectiveness at capturing complex relationships between channels and temporal dynamics. Conversely, simple MLP-based models, including DLinear (Zeng et al., 2023) and TSMixer (Chen et al., 2023), have demonstrated that MLPs are already capable of learning these intricate interdependencies between channels and time steps.

Extensive research has focused on enhancing model capacity to capture intricate temporal and channel dynamics within multivariate data. PatchTST (Nie et al., 2023) successfully adapted the patching mechanism originally proposed for Vision Transformers (Dosovitskiy et al., 2021), processing time series as sequences of localized segments rather than individual points. This shift enables the model to extract meaningful local semantics as grouping adjacent time steps into tokens that preserve structural patterns and reduce the noise inherent at the single-step level.

The majority of recent studies incorporate patching techniques utilizing overlapping patches, a method wherein a sliding window moves across the time series with a stride smaller than the patch length. While this approach has the potential to more deeply capture local semantics by providing the model with multiple perspectives of the same temporal points, it inherently increases computational overhead. Furthermore, high degrees of overlap resulting from excessively small strides can introduce redundant information rather than meaningful features, potentially leading to inefficient learning and increased risk of overfitting.

In this paper, we propose a non-overlapping patching framework that aggregates neighboring patches in a hierarchical manner. As the model facilitates learning between adjacent patches across successive levels of the hierarchy, it effectively captures both local semantics and broader global context in the hierarchical mechanism.

Several recent studies propose performing time series forecasting within the frequency domain. By applying transformations such as the Fast Fourier Transform (FFT) (Yi et al., 2023; Cai et al., 2024) or Wavelet Transform (Yang et al., 2023; Chen et al., 2025), models decompose complex signals into constituent periodic components. This approach helps the network isolate seasonal patterns and noise from

---

<sup>1</sup>ISMILL, University of Hildesheim, VWFS Data Analytics Research Center (VWFS-DARC), Hildesheim, Germany. Correspondence to: Jung Min Choi <choi@ismll.de>, Vijaya Krishna Yalavarthi <yalavarthi@ismll.de>, Lars Schmidt-Thieme <schmidt-thieme@ismll.de>.

the primary trend. Consequently, the model can analyze global periodicities that are often difficult to discern in the raw time domain (Zhou et al., 2022).

Our model utilizes a Learnable Stationary Wavelet Transform (LSWT) (Michau et al., 2022). This framework optimizes filter coefficients during training to adaptively capture multiscale temporal features. Unlike the Discrete Wavelet Transform (DWT) (Heil & Walnut, 1989), the Stationary Wavelet Transform (SWT) omits downsampling. This preserves the original sequence length and maintains translation invariance (Nason & Silverman, 1995).

Our proposed model, **Neighboring Patching Mixer (NPMixer)**, is a simple yet effective architecture. It is designed to capture seasonality and trends through multiscale frequency coefficients. The core of the model is a recursive pairing strategy that facilitates multi-scale interaction between adjacent, non-overlapping patches. This enables the efficient extraction of complex temporal patterns across multiple resolutions. The hierarchical pairing process is executed within the frequency domain using components decomposed by the LSWT. This allows the model to isolate and process specific periodicities and noise patterns independently across different scales.

To achieve this, we introduce the Neighboring Mixer Block, which employs an iterative “Group-Mix-Dissolve” strategy. At each level of the hierarchy, adjacent temporal blocks are paired and processed through a shared relational MLP to expand the receptive field. These pairs are then dissolved and regrouped, allowing the network to dynamically integrate fine-grained local semantics into a comprehensive global representation. Through this multi-resolution approach, NPMixer effectively distinguishes between transient local fluctuations and persistent global trends without the redundancy of dense sliding windows.

The main contributions of this paper are as follows:

1. We demonstrate that recursive patch aggregation effectively captures the transition from local granular details to global temporal dependencies, enriching the model’s ability to represent multi-scale dynamics.
2. We show that multi-scale learning within the frequency domain is crucial for time series forecasting to capture precise temporal dynamics across different resolutions.
3. We propose **NPMixer**, a simple yet effective architecture that achieves state-of-the-art results across various multivariate time series datasets for long-term time series forecasting tasks.

## 2. Related Works

**Time Series Forecasting.** Current TSF architectures are primarily categorized into MLP, Transformer, CNN, and GNN-based models. MLP-based models, such as TSMixer (Chen et al., 2023) and DLinear (Zeng et al., 2023), are favored for their computational efficiency. Recent advancements like TimeMixer (Wang et al., 2024a) further enhance this by incorporating multi-scale decomposition to handle structural variations.

Transformer (Vaswani et al., 2017)-based models utilize self-attention to capture long-range dependencies, with PatchTST (Nie et al., 2023) introducing patching for local semantic extraction and iTransformer (Liu et al., 2024) focusing on multivariate correlations. CNN-based models, such as MICN (Wang et al., 2023), employ multi-scale kernels to extract hierarchical patterns. Finally, GNN-based models like MSGNet (Cai et al., 2024) and WaveForM (Yang et al., 2023) represent variables as nodes to adaptively learn complex spatial-temporal correlations across diverse resolutions.

**Patching in TSF.** Originally inspired by the Vision Transformer (Dosovitskiy et al., 2021), patching in TSF involves segmenting a continuous sequence into sub-series tokens. This approach shifts the model’s focus from individual point-wise observations to local semantic patterns, significantly reducing the input token length for long-sequence tasks. PatchTST (Nie et al., 2023) utilized this by treating patches as independent tokens within a Transformer backbone to capture local temporal context. Furthermore, TSMixer (Ekambaram et al., 2023) extended this concept by employing intra-patch and inter-patch mixing to extract dependencies within and across these segments. While most models utilize overlapping windows to preserve continuity, the Swin Transformer (Liu et al., 2021) demonstrated the efficiency of non-overlapping windows in computer vision, utilizing hierarchical merging to build a global receptive field. Inspired by this, our model adopts a non-overlapping patching strategy for time series, achieving multi-scale representation through hierarchical pairing without the computational redundancy of overlapping strides.

**Frequency Domain in TSF.** Transforming time-series data into the frequency domain allows models to uncover latent periodicities and cyclical patterns often obscured in the time domain. FEDformer (Zhou et al., 2022) utilizes the Discrete Fourier Transform (DFT) to process frequency spectra within its attention mechanism, while FreTS (Yi et al., 2023) utilizes a frequency-domain MLP architecture by applying the FFT. It learns multivariate correlations and global dependencies through specialized frequency-channel and frequency-temporal MLPs. Other approaches, such as WaveForM (Yang et al., 2023), incorporate the DWT to analyze signals at varying resolutions. However, the

downsampling inherent in DWT breaks shift-invariance, potentially leading to feature loss. To address this, SimpleTM (Chen et al., 2025) employs the LSWT, which preserves translation invariance and enables the data-driven optimization of decomposition layers. Our model integrates this LSWT approach to provide a stable, high-fidelity frequency foundation for our hierarchical pairing patching mechanism across all temporal shifts.

### 3. Methodology

In this section, we present the architecture of **NPMixer**, which consists of three core components designed to capture multi-scale temporal dynamics and cross-channel correlations. First, the **Learnable Stationary Wavelet Transform/Inverse Wavelet Transform (SWT/ISWT)** module adaptively optimizes wavelet filter coefficients to decompose the input into robust frequency sub-coefficients. Second, the **Neighboring Mixer Blocks** facilitate hierarchical interaction between adjacent, non-overlapping patches to extract both local semantics and global context. Finally, the **Channel-Mixing Encoder**, alongside **Single- and Multi-Patch MLPs**, serves to learn intricate interdependencies within patches and across the multivariate feature space. The comprehensive framework is illustrated in Figure 1.

#### 3.1. Preliminaries

Consider an Multivariate Time Series (MTS) containing  $C$  variables recorded across a historical look-back window of length  $L$ . This input is defined as a matrix  $\mathbf{X} \in \mathbb{R}^{C \times L}$ , where each column vector  $\mathbf{x}_t = [x_{t,1}, x_{t,2}, \dots, x_{t,C}]^\top \in \mathbb{R}^C$  denotes the collective observations at index  $t$ . The primary objective of MTS forecasting is to utilize the past sequence  $\mathbf{X}$  to estimate future values over a pre-determined horizon  $H$ . We denote the target future values as  $\mathbf{Y} \in \mathbb{R}^{C \times H}$ , representing the subsequent  $H$  time steps. Formally, our goal is to develop a predictive mapping  $\mathcal{F} : \mathbb{R}^{C \times L} \rightarrow \mathbb{R}^{C \times H}$  that minimizes the discrepancy between the estimated output  $\hat{\mathbf{Y}}$  and the ground truth  $\mathbf{Y}$ .

#### 3.2. Learnable SWT/ISWT

To decompose the input series into multi-resolution frequency sub-bands, we employ a *Learnable Stationary Wavelet Transform (LSWT)*. While standard wavelets such as Haar or Daubechies rely on fixed basis functions, parameterizing the filters as trainable tensors allows the decomposition to adapt dynamically to the specific spectral characteristics of the data (Michau et al., 2022).

We adopt this fully learnable framework to optimize feature extraction for the forecasting task. The LSWT performs a translation-invariant decomposition by convolving the input signal with pairs of low-pass ( $\mathbf{h}_0$ ) and high-pass ( $\mathbf{h}_1$ ) fil-

ters. Unlike the standard discrete wavelet transform (DWT), the SWT utilizes dilated convolutions to preserve the full temporal resolution  $L$  at every level. Consequently, a decomposition of depth  $M$  results in  $M + 1$  distinct sub-band components: one global approximation coefficient  $\mathbf{A}_M$  and  $M$  multi-scale detail coefficients  $\{\mathbf{D}_m\}_{m=1}^M$ .

We initialize the filters using a reference wavelet basis  $\mathbf{W}_{\text{init}}$  (e.g., db1) to ensure stability at the start of training, but allow them to evolve freely via backpropagation:

$$\mathbf{h}_0 = \mathbf{W}_{\text{init}}^{\text{lo}} + \Delta\theta^{\text{lo}}, \quad \mathbf{h}_1 = \mathbf{W}_{\text{init}}^{\text{hi}} + \Delta\theta^{\text{hi}} \quad (1)$$

where  $\Delta\theta$  represents the learnable parameter updates. This flexibility allows the model to deviate from rigid mathematical constraints, effectively learning a task-specific spectral basis that minimizes the global forecasting error.

The forward decomposition begins by treating the input time series  $\mathbf{X}$  as the initial approximation  $\mathbf{A}_0$ . At each subsequent level  $m$ , the coefficients are computed recursively:

$$\mathbf{A}_m = \mathbf{A}_{m-1} *_{d_m} \mathbf{h}_0 \quad (2)$$

$$\mathbf{D}_m = \mathbf{A}_{m-1} *_{d_m} \mathbf{h}_1 \quad (3)$$

where  $*_{d_m}$  denotes a convolution with dilation factor  $d_m = 2^{m-1}$ .

Correspondingly, the signal is reconstructed via a Learnable Inverse SWT (LISWT), which sums the dilated convolutions of the coefficients with adaptive synthesis filters  $\mathbf{g}_0, \mathbf{g}_1$ :

$$\mathbf{A}_{m-1} = \frac{1}{2} (\mathbf{A}_m *_{d_m} \mathbf{g}_0 + \mathbf{D}_m *_{d_m} \mathbf{g}_1) \quad (4)$$

The LSWT operates as an adaptive feature extractor by integrating a learnable decomposition framework. This allows the network to partition signal components into a single long-term trend,  $\mathbf{A}_M$ , and a set of multi-scale transient fluctuations,  $\{\mathbf{D}_m\}_{m=1}^M$ . This disentanglement exposes temporal patterns that are not explicitly separable in the raw time domain, facilitating more effective processing in the subsequent mixing layers.

#### 3.3. Channel-Mixing Encoder

The detail coefficients  $\mathbf{D}_m$  often contain high-frequency fluctuations that are strongly correlated across different variables. To capture these multivariate dependencies, we incorporate a *Channel-Mixing Encoder* applied exclusively to the detail branches ( $m < K$ ).

Adopting the inverted architecture proposed in iTransformer (Liu et al., 2024), we treat the entire look-back series of each variate as a distinct token. For a detail coefficient  $\mathbf{D}_m \in \mathbb{R}^{C \times L}$ , we embed the temporal dimension  $L$  into a latent feature space  $d_{\text{model}}$ :

$$\mathbf{H}_{m,0} = \text{Embed}(\mathbf{D}_m) \in \mathbb{R}^{C \times d_{\text{model}}} \quad (5)$$

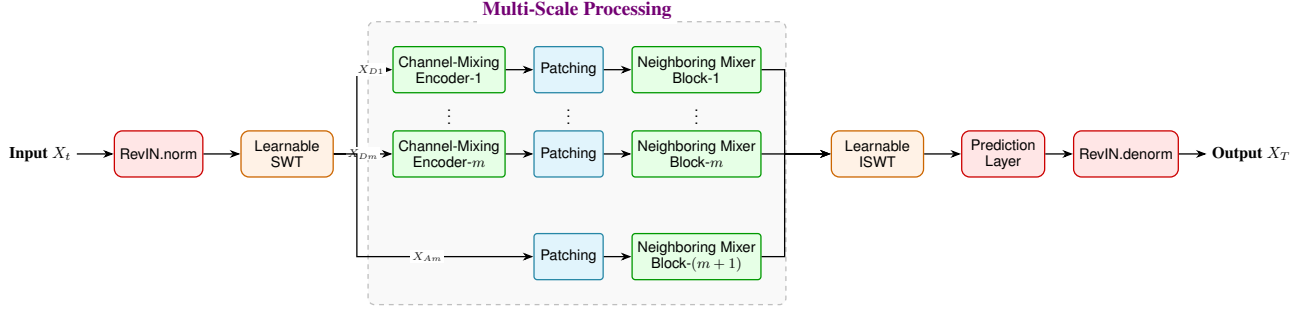


Figure 1. The overall architecture of NPMixer. The input sequence is decomposed via Learnable SWT. Detail coefficients ( $X_D$ ) are processed via Channel-Mixing Encoders and Neighboring Mixer Blocks, while the approximate coefficient ( $X_A$ ) skips the encoder to preserve trend information. Features are reconstructed via ISWT for the final forecast.

where  $C$  denotes the number of variates. For notational convenience, we hereafter omit the scale index  $m$  and denote the initial hidden representation as  $\mathbf{H}_0$  when referring to the input of the mixing layers.

These tokens are processed by a standard Transformer encoder. Since the attention mechanism operates across the  $C$  dimension, the self-attention map explicitly models the pairwise correlations between variables, learning a dynamic graph of multivariate interactions:

$$\mathbf{H}_{l+1} = \text{FeedForward}(\text{MSA}(\mathbf{H}_l)) \quad (6)$$

where MSA denotes Multi-Head Self-Attention. This allows the model to refine the high-frequency features of one variable based on the state of correlated variables.

Finally, a projection layer maps the latent representation back to the original sequence length  $L$ , and a residual connection restores the original signal scale:

$$\hat{\mathbf{D}}_m = \mathbf{D}_m + \text{Project}(\mathbf{H}_{\text{last}}) \quad (7)$$

Notably, we exclude this encoder from the approximation branch ( $\mathbf{A}_K$ ), as the low-frequency trend is better modeled by preserving its smooth, univariate trajectory without the noise of cross-channel mixing.

### 3.4. Non-Overlapping Patching and Neighboring Mixer Block

The Neighboring Mixer Block captures multi-scale temporal dependencies through a hierarchical pairing strategy. Our approach utilizes non-overlapping patches and recursively processes adjacent blocks to expand the receptive field efficiently. By pairing neighboring temporal segments at each successive layer, the model transitions from learning local granular features to capturing global sequence-wide patterns without the redundancy of dense sliding windows. The detailed structure of this hierarchical pairing mechanism is illustrated in Figure 2.

**Non-overlapping Patching** Given the input time series or its decomposed sub-band coefficients  $\mathbf{X} \in \mathbb{R}^{C \times L}$ , the sequence is divided into  $N$  non-overlapping patches of length  $P$ . We apply zero-padding to the end of the sequence to ensure the length  $L$  is exactly divisible by  $P$ . The padding length  $L_{pad}$  represents the space required to complete the final patch. This value is zero if the input is already perfectly divisible. Following this adjustment, the sequence is reshaped into  $\mathbf{X}_p \in \mathbb{R}^{C \times N \times P}$ , where  $N = (L + L_{pad})/P$  denotes the total number of patches.

**Single-Patch MLP** Before hierarchical mixing, a Single-Patch MLP is applied to each patch independently to extract local feature representations. We employ a two-layer MLP with GELU activation, adding the refined features back to the input via a residual connection:

$$\mathbf{X}'_p = \mathbf{X}_p + \text{SP-MLP}(\mathbf{X}_p) \quad (8)$$

This treats every patch as an isolated sample, ensuring that raw temporal information is preserved while learning internal dynamics.

**Neighboring Mixer Block and Multi-Patch MLP** To expand the temporal receptive field, the model employs an iterative *Group-Mix-Dissolve* strategy. At each level  $k$ , the sequence is reshaped into discrete blocks of size  $S_k = 2^{k-1}P$ .

We generate relational features by processing overlapping pairs of adjacent blocks  $[\mathbf{q}_i \parallel \mathbf{q}_{i+1}]$  through a deep Multi-Patch MLP. This module consists of a stack of  $n$  fully connected layers utilizing GELU activations and dropout. This depth allows the model to learn complex, high-order dependencies between neighboring windows:

$$\mathbf{R}_i = \text{MP-MLP}([\mathbf{q}_i \parallel \mathbf{q}_{i+1}]; \theta_k) \quad (9)$$

where MP-MLP( $\cdot$ ) denotes the deep projection network and  $\theta_k$  represents the learnable weights at hierarchy level  $k$ .

To optimize for forecasting, we regulate the information flow direction via a learnable gate  $\alpha_k = \sigma(\gamma_k) \in (0, 1)$ .

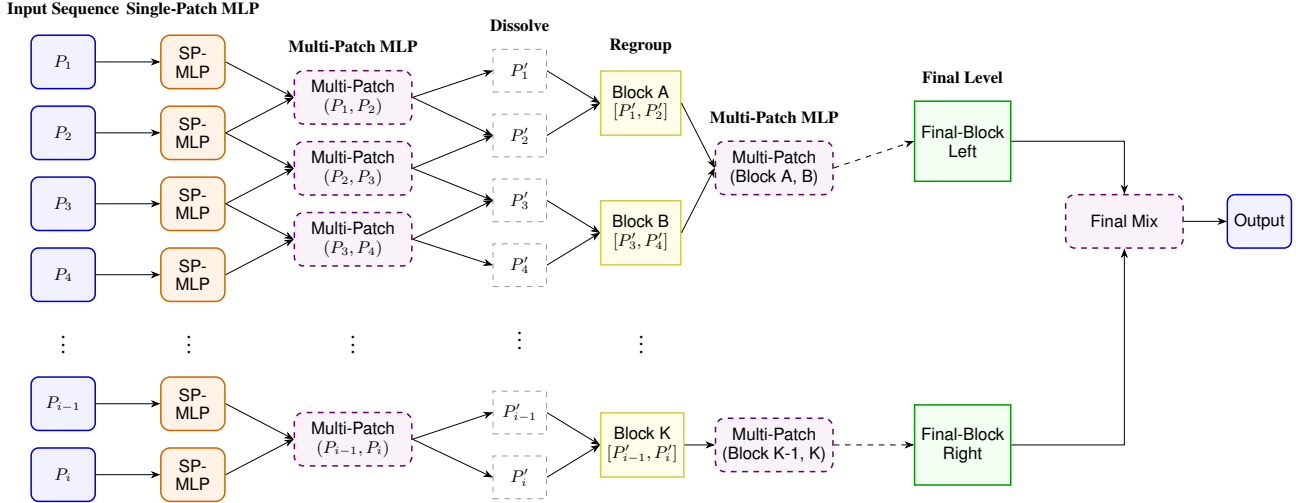


Figure 2. The Architecture of the *Neighboring Mixer Block*.

Building on the findings of Gontijo-Lopes et al. (Gontijo-Lopes et al., 2021), which suggest that representation power is maximized when components specialize in distinct data subdomains, we implement an asymmetric update strategy. Rather than applying symmetric mixing, we enforce a directional bias that aligns with the temporal structure of forecasting.

Specifically, we design the residual connections to fulfill specialized roles depending on their position in the sequence. The initial block  $\mathbf{q}_0$  is dedicated to capturing future-oriented signals, updating solely based on its interaction with the subsequent block. Conversely, for the remainder of the sequence ( $i > 0$ ), we prioritize historical continuity by integrating relationships exclusively from the preceding context:

$$\mathbf{q}_i^{(\text{new})} = \begin{cases} \mathbf{q}_0 + \alpha_k \cdot \mathbf{R}_0 & \text{if } i = 0 \\ \mathbf{q}_i + (1 - \alpha_k) \cdot \mathbf{R}_{i-1} & \text{if } i > 0 \end{cases} \quad (10)$$

This design effectively anchors the start of the sequence with anticipatory information while ensuring that the subsequent trajectory is stabilized by autoregressive dependencies.

### 3.5. Final Projection

The *Final Projection* layer maps refined representations to the forecasting horizon  $H$ . This layer operates in the time domain to integrate global temporal dependencies. We apply a global bottleneck transformation across the sequence length  $L$  and use a residual connection to generate the final forecast  $\mathbf{Y} \in \mathbb{R}^{C \times H}$ . The process is followed by RevIN de-normalization (Kim et al., 2022) and is defined as:

$$\mathbf{Y} = \left( \hat{\mathbf{X}} + \text{GELU}(\hat{\mathbf{X}}\mathbf{W}_g + \mathbf{b}_g) \right) \mathbf{W}_{out} + \mathbf{b}_{out} \quad (11)$$

where  $\mathbf{W}_g \in \mathbb{R}^{L \times L}$  and  $\mathbf{W}_{out} \in \mathbb{R}^{L \times H}$  are learnable weights.

## 4. Experiments

### 4.1. Experimental Setup

**Datasets and Baseline Models** The efficacy of NPMixer is validated through comprehensive experiments on seven standard time series forecasting benchmarks: ETTh1, ETTh2, ETTm1, ETTm2, Weather, Electricity, and Traffic (Zhou et al., 2021). These datasets encompass diverse real-world domains with varying temporal frequencies and channel counts, providing a robust environment to test the model’s generalization capabilities across different data characteristics. We establish a competitive baseline by comparing our model against six recent state-of-the-art architectures in multivariate time series forecasting, including SimpleTM (Chen et al., 2025), Timexer (Wang et al., 2024b), CrossGNN (Huang et al., 2023), iTransformer (Liu et al., 2024), PatchTST (Nie et al., 2023), and TimeMixer (Wang et al., 2024a).

**Evaluation Protocols** Our evaluation focuses on long-term forecasting scenarios across four standard horizons:  $H \in \{96, 192, 336, 720\}$ . We follow the same data processing and splitting protocols as described in (Wu et al., 2023). The look-back window length is fixed at  $L = 96$  for all datasets. During the training phase, we optimize the network by minimizing the Mean Squared Error (MSE). For a robust assessment of performance on the test set, we report both the MSE and the Mean Absolute Error (MAE).

### 4.2. Main Results

As demonstrated in Table 1, NPMixer consistently outperforms the other baseline models across the majority of benchmark datasets, securing the highest overall win count with 20 best results in MSE and 18 in MAE among specific prediction horizons. The model exhibits a particularly signif-

Table 1. Full results over different horizons on the standard datasets. The results are an average of three different random seeds. The best variant for each model is in **bold** and the second best model is in Underline. The MSE/MAE values for the baselines are imported from (Chen et al., 2025), (Liu et al., 2024), and (Wang et al., 2024a).

Dataset	Horizon	NPMixer (Ours)		SimpleTM		TimeXer		CrossGNN		iTransformer		PatchTST		TimeMixer	
		MSE	MAE	MSE	MAE	MSE	MAE	MSE	MAE	MSE	MAE	MSE	MAE	MSE	MAE
ETTh1	96	<b>0.306</b>	<b>0.348</b>	0.321	0.361	<u>0.318</u>	<u>0.356</u>	0.335	0.373	0.334	0.368	0.329	0.367	0.328	0.363
	192	<b>0.344</b>	<b>0.373</b>	<u>0.360</u>	<u>0.380</u>	0.362	0.383	0.372	0.390	0.377	0.391	0.367	0.385	0.364	0.384
	336	<b>0.370</b>	<b>0.395</b>	<u>0.389</u>	<u>0.403</u>	0.395	0.407	0.403	0.411	0.426	0.420	0.399	0.410	0.390	0.404
	720	<b>0.431</b>	<b>0.429</b>	0.454	<u>0.438</u>	0.452	0.441	0.461	0.442	0.491	0.459	0.454	0.439	0.458	0.445
	Avg	<b>0.362</b>	<b>0.386</b>	<u>0.381</u>	<u>0.396</u>	0.382	0.397	0.393	0.404	0.407	0.410	0.387	0.400	0.385	0.399
ETTh2	96	<b>0.166</b>	<b>0.250</b>	0.173	0.257	<u>0.171</u>	<u>0.256</u>	0.176	0.266	0.180	0.264	0.175	0.259	0.176	0.259
	192	<b>0.234</b>	<b>0.296</b>	0.238	<u>0.299</u>	<u>0.237</u>	<u>0.299</u>	0.240	0.307	0.250	0.309	0.241	0.302	0.242	0.303
	336	<b>0.291</b>	<b>0.332</b>	<u>0.296</u>	<u>0.338</u>	<u>0.296</u>	<u>0.338</u>	0.304	0.345	0.311	0.348	0.305	0.343	0.304	0.342
	720	<b>0.390</b>	<b>0.390</b>	<u>0.393</u>	0.395	<u>0.392</u>	<u>0.394</u>	0.406	0.400	0.412	0.407	0.402	0.400	<u>0.393</u>	0.397
	Avg	<b>0.270</b>	<b>0.317</b>	0.278	0.325	<u>0.274</u>	<u>0.322</u>	0.282	0.330	0.288	0.332	0.281	0.326	0.278	0.325
ETTh1	96	<b>0.361</b>	<b>0.392</b>	<u>0.366</u>	<b>0.392</b>	0.382	0.403	0.382	0.398	0.386	0.405	0.414	0.419	0.381	0.401
	192	<b>0.419</b>	0.429	<u>0.422</u>	<b>0.421</b>	0.429	0.435	0.427	<u>0.425</u>	0.441	0.436	0.460	0.445	0.440	0.433
	336	<u>0.455</u>	0.451	<b>0.440</b>	<b>0.438</b>	0.468	0.448	0.465	<u>0.445</u>	0.487	0.458	0.501	0.466	0.501	0.462
	720	<b>0.458</b>	<b>0.461</b>	<u>0.463</u>	<u>0.462</u>	0.469	<b>0.461</b>	0.472	0.468	0.503	0.491	0.500	0.488	0.501	0.482
	Avg	<u>0.423</u>	<u>0.433</u>	<b>0.422</b>	<b>0.428</b>	0.437	0.437	0.437	0.434	0.454	0.447	0.469	0.454	0.458	0.445
ETTh2	96	<b>0.280</b>	<b>0.337</b>	<u>0.281</u>	<u>0.338</u>	0.286	<u>0.338</u>	0.309	0.359	0.297	0.349	0.302	0.348	0.292	0.343
	192	<b>0.354</b>	<b>0.383</b>	<u>0.355</u>	<u>0.387</u>	0.363	0.389	0.390	0.406	0.380	0.400	0.388	0.400	0.374	0.395
	336	<u>0.404</u>	0.424	<b>0.365</b>	<b>0.401</b>	0.414	<u>0.423</u>	0.426	0.444	0.428	0.432	0.426	0.433	0.428	0.433
	720	<b>0.407</b>	<b>0.430</b>	0.413	0.436	<u>0.408</u>	<u>0.432</u>	0.445	0.464	0.427	0.445	0.431	0.446	0.454	0.458
	Avg	<u>0.361</u>	<u>0.393</u>	<b>0.353</b>	<b>0.391</b>	0.367	0.396	0.393	0.413	0.383	0.407	0.387	0.407	0.384	0.407
Electricity	96	<b>0.138</b>	<b>0.235</b>	0.141	<b>0.235</b>	<u>0.140</u>	0.242	0.173	0.275	0.148	<u>0.240</u>	0.181	0.270	0.153	0.244
	192	<u>0.155</u>	<u>0.251</u>	<b>0.151</b>	<b>0.247</b>	0.157	0.256	0.195	0.288	0.162	0.253	0.188	0.274	0.166	0.256
	336	<b>0.172</b>	<b>0.267</b>	0.173	<b>0.267</b>	0.176	0.275	0.206	0.3	0.178	<u>0.269</u>	0.204	0.293	0.184	0.275
	720	<u>0.205</u>	<u>0.299</u>	<b>0.201</b>	<b>0.293</b>	0.211	0.306	0.231	0.335	0.225	0.317	0.246	0.324	0.226	0.313
	Avg	<u>0.167</u>	<u>0.263</u>	<b>0.166</b>	<b>0.260</b>	0.171	0.270	0.201	0.3	0.178	0.270	0.205	0.290	0.182	0.272
Weather	96	<b>0.154</b>	<b>0.202</b>	0.162	0.207	<u>0.157</u>	<u>0.205</u>	0.159	0.218	0.174	0.214	0.177	0.218	0.165	0.212
	192	<b>0.204</b>	<u>0.248</u>	0.208	<u>0.248</u>	<b>0.204</b>	<b>0.247</b>	<u>0.211</u>	0.266	0.221	0.254	0.225	0.259	0.209	0.253
	336	<b>0.261</b>	<b>0.287</b>	0.263	0.290	<b>0.261</b>	<u>0.290</u>	0.267	0.31	0.278	0.296	0.278	0.297	0.264	0.293
	720	<b>0.340</b>	<b>0.338</b>	<b>0.340</b>	<u>0.341</u>	<b>0.340</b>	<u>0.341</u>	0.352	0.362	0.358	0.347	0.354	0.348	0.342	0.345
	Avg	<b>0.239</b>	<b>0.268</b>	0.243	<u>0.271</u>	<u>0.241</u>	<u>0.271</u>	0.247	0.289	0.243	<u>0.271</u>	0.259	0.281	0.245	0.276
Traffic	96	<u>0.404</u>	0.279	0.410	<u>0.274</u>	0.428	0.271	0.570	0.310	<b>0.395</b>	<b>0.268</b>	0.462	0.295	0.464	0.289
	192	0.433	0.293	<u>0.430</u>	<u>0.280</u>	0.448	0.282	0.577	0.321	<b>0.417</b>	<b>0.276</b>	0.466	0.296	0.477	0.292
	336	<u>0.449</u>	0.301	<u>0.449</u>	0.290	0.473	<u>0.289</u>	0.588	0.324	<b>0.433</b>	<b>0.283</b>	0.482	0.304	0.500	0.305
	720	<u>0.484</u>	0.317	0.486	0.309	0.516	<u>0.307</u>	0.597	0.337	<b>0.467</b>	<b>0.302</b>	0.514	0.322	0.548	0.313
	Avg	0.442	0.297	<u>0.444</u>	0.289	0.466	<u>0.287</u>	0.583	0.323	<b>0.428</b>	<b>0.282</b>	0.481	0.304	0.484	0.297
<b>Win Count</b>		<b>20</b>	<b>18</b>	<u>5</u>	<u>8</u>	3	2	0	0	4	4	0	0	0	0

icant performance lift on the ETTh1 and ETTh2 datasets. For instance, on ETTh1, NPMixer delivers a 4.98% improvement in average MSE over the second-best variant, SimpleTM. While SimpleTM also incorporates a LSMT, our architecture’s distinct integration of non-overlapping patching and the hierarchical Neighboring Mixer Block

yields better feature extraction capabilities. This structural advantage is empirically evident in the ETTh1 and ETTh2 benchmarks, where NPMixer demonstrates robust improvements over SimpleTM. Notably, on the ETTh2 dataset, our model achieves the lowest MSE across the 96, 192, and 720 horizons. Furthermore, in the challenging long-term

Table 2. Comparison of Average Performance (MSE and MAE) across standard datasets. Results are averaged over all prediction horizons ( $H \in \{96, 192, 336, 720\}$ ) and across three different random seeds. For each model, the look-back window size was independently tuned from  $\{96, 192, 336, 512\}$  to ensure a fair comparison. Baseline results are sourced from TimeMixer (Wang et al., 2024a), Crossformer (Zhang & Yan, 2023) and DLinear (Zeng et al., 2023). The best results are in **bold** and the second-best results are underlined. The full results are provided in Table 10 of Appendix B.

Dataset	NPMixer (Ours)		TimeMixer		PatchTST		TSMixer		TimesNet		Crossformer	
	MSE	MAE	MSE	MAE	MSE	MAE	MSE	MAE	MSE	MAE	MSE	MAE
ETTm1	<b>0.343</b>	<u>0.377</u>	<u>0.348</u>	<b>0.375</b>	0.353	0.382	0.347	0.375	0.400	0.406	0.514	0.510
ETTm2	<b>0.251</b>	<b>0.312</b>	<u>0.256</u>	<u>0.315</u>	0.256	0.317	0.267	0.322	0.291	0.333	0.621	0.510
ETTh1	<b>0.409</b>	<u>0.426</u>	<u>0.411</u>	<b>0.423</b>	0.413	0.434	0.412	0.428	0.458	0.450	0.600	0.557
ETTh2	0.335	0.388	<b>0.316</b>	<u>0.384</u>	<u>0.331</u>	<b>0.381</b>	0.355	0.401	0.414	0.427	0.564	0.548
Electricity	<b>0.155</b>	<b>0.239</b>	<u>0.156</u>	<u>0.246</u>	0.159	0.253	0.160	0.257	0.192	0.295	0.186	0.283
Weather	<b>0.215</b>	<b>0.254</b>	<u>0.222</u>	<u>0.262</u>	0.226	0.264	0.225	0.264	0.259	0.287	0.406	0.442
Traffic	<u>0.391</u>	0.269	<b>0.387</b>	<b>0.262</b>	<u>0.391</u>	<u>0.264</u>	0.408	0.284	0.620	0.336	0.542	0.283
<b>Win Count</b>	<b>5</b>	<b>3</b>	<u>2</u>	<b>3</b>	0	1/7	0	0	0	0	0	0

forecasting scenario of ETTh1 ( $H = 720$ ), NPMixer surpasses SimpleTM, confirming that our future-oriented relational mixing provides greater stability and predictive accuracy over extended temporal scales compared to the standard LSWT approach. In the high-dimensional Traffic dataset, while iTransformer maintains its dominance in modeling complex channel correlations, NPMixer consistently reaches the second-best performance, underscoring its versatility. These results validate that the synergy between learnable spectral decomposition and hierarchical temporal mixing allows NPMixer to effectively capture local details with global context, establishing a new state-of-the-art for multivariate time series forecasting.

### 4.3. Look-Back Window Analysis

In this section, we investigate the impact of look-back window tuning on model performance across various benchmarks. Table 2 presents the average results obtained after independently optimizing the input sequence length for each model. The tuning of the look-back window is a critical requirement for ensuring experimental fairness and avoiding biased comparisons between forecasting architectures (Qiu et al., 2024). Previous studies, such as PatchTST (Nie et al., 2023), have demonstrated that certain architectures are highly sensitive to input length, often achieving significantly better results with longer sequences (e.g.,  $L = 336$ ) compared to the standard  $L = 96$ . By exploring various look-back lengths, we provide a more rigorous comparison that accounts for the maximum potential of each architecture.

Our model demonstrates better performance in 5 out of 7 standard public datasets under optimal window settings. Notably, the model exhibits a significant performance lift in the Electricity and Weather datasets. While the improvement in the Electricity dataset was more moderate at the fixed

$L = 96$  setting, window tuning reveals its capacity, where NPMixer achieves the lowest MSE of 0.155 and MAE of 0.239. Similarly, in the Weather dataset, NPMixer outperforms all competitors with a significant margin, achieving an MSE of 0.215.

These results underscore the robustness of NPMixer when dealing with long look-back windows. It can be attributed to our hierarchical block-mixing strategy as the look-back window size grows, the model benefits from a larger number of patches, which allows for a more granular decomposition of local features and a more comprehensive hierarchical aggregation of global context. This suggests that NPMixer is effectively equipped to exploit the richer historical information present in extended input horizons.

### 4.4. Ablation Study

We conduct a comprehensive ablation study across seven benchmark datasets. The results, summarized in Table 3, demonstrate that NPMixer achieves the better performance in nearly all scenarios. We compare our approach against a w/o Neighboring Mixer variant, which utilizes only a single-patch mixer and the final projection layer that processes all patches simultaneously. The results indicate that removing the intermediate hierarchical pairing leads to significant degradation in accuracy. For instance, in the Traffic and ETTh1 datasets, the absence of the multi-level structure results in an MSE increase of 18.01% and 6.63%, respectively. This highlights that the recursive block-mixing strategy is essential for systematically capturing dependencies that exist between local granular details and the global temporal context.

Similarly, the Channel-Mixing Encoder proves cruciality for handling multivariate relationships. Its impact is most pronounced in high-dimensional datasets. In the Traffic

Table 3. Ablation study results across all datasets. Results are averaged over all prediction horizons ( $H \in \{96, 192, 336, 720\}$ ) and across three different random seeds. The variants are defined as follows: (1) **w/o SWT**: Removes the wavelet decomposition, forcing the model to operate entirely in the time domain without multi-resolution features. (2) **w/o Learnable SWT**: Utilizes standard SWT with fixed coefficients instead of data-dependent learnable filters. (3) **w/o Neighboring Mixer**: Removes the neighboring patch-pairing strategy, relying only on the channel-mixing encoder, single-patch MLP, and global MLP. (4) **w/o Channel-Mixing Encoder**: Excludes the self-attention mechanism, thereby removing explicit cross-channel correlation modeling. The full results are provided in Table 9 of Appendix B.

Model	ETTm1		ETTm2		ETTh1		ETTh2		ECL		Weather		Traffic	
	MSE	MAE	MSE	MAE	MSE	MAE	MSE	MAE	MSE	MAE	MSE	MAE	MSE	MAE
w/o SWT	0.371	0.388	0.274	<u>0.319</u>	<u>0.429</u>	<u>0.431</u>	0.375	0.400	0.172	0.265	0.249	0.274	<b>0.442</b>	<b>0.297</b>
w/o Learnable SWT	<u>0.365</u>	<u>0.387</u>	<u>0.273</u>	0.320	0.443	0.441	<u>0.369</u>	<u>0.397</u>	<u>0.171</u>	<u>0.266</u>	0.245	<u>0.272</u>	0.449	<u>0.300</u>
w/o Neighboring Mixer	0.386	0.402	0.279	0.324	0.455	0.447	0.383	0.406	0.188	0.288	<u>0.242</u>	<u>0.273</u>	0.522	0.356
w/o Channel-Mixing Encoder	0.371	0.391	0.275	0.321	0.453	0.442	0.370	0.399	0.183	0.274	<u>0.242</u>	<u>0.272</u>	0.518	0.334
NPMixer	<b>0.362</b>	<b>0.386</b>	<b>0.270</b>	<b>0.317</b>	<b>0.423</b>	<u>0.433</u>	<b>0.361</b>	<b>0.393</b>	<b>0.167</b>	<b>0.263</b>	<b>0.240</b>	<b>0.269</b>	<b>0.442</b>	<b>0.297</b>

dataset, removing the encoder leads to a 17.19% increase in MSE. This suggests that explicitly modeling inter-channel correlations in the high-frequency domain is essential when the number of variables is large, as it provides a globally-informed foundation for the subsequent temporal mixing stages.

Overall, the learnable aspect of the decomposition also remains significant. LSWT provides a consistent performance lift, particularly in ETTm1 and Weather datasets, where it reduces average MSE by approximately 0.82% and 2.04%, respectively.

Interestingly, for the Traffic dataset, we observe that the variant without the Stationary Wavelet Transform (w/o SWT) achieves performance identical to the full NPMixer model. Given the extreme dimensionality of this dataset (862 features), this suggests that the benefits of frequency-domain decomposition may be marginal in such high-dimensional contexts. It is possible that the sheer volume of features already provides sufficient representational capacity for temporal mixing, or that the additional complexity introduced by spectral separation does not provide further discriminative power for this specific data structure.

## 5. Conclusion and Future Work

In this paper, we introduced NPMixer, a novel MTS forecasting architecture that effectively learns local temporal dynamics alongside global dependencies through a hierarchical mixing strategy. By leveraging a LSWT, our model adaptively decomposes complex signals into trend and detail components, allowing for specialized feature extraction across distinct frequency sub-bands. The integration of the Channel-Mixing Encoder specifically for detail coefficients ensures that cross-variable correlations are captured without destabilizing the underlying global trajectory of the series.

Our extensive experiments across seven benchmark datasets

demonstrate that NPMixer achieves state-of-the-art performance, securing the highest win count in both MSE and MAE. The hierarchical block-mixing mechanism proves effective for long-term forecasting, as evidenced by our look-back window analysis.

Despite these advancements, we acknowledge several limitations inherent to the model’s design. First, the hierarchical aggregation relies on exponential block sizing ( $S_k = 2^{k-1}P$ ), which imposes strict constraints on input lengths. This often necessitates zero-padding, which can introduce distributional shifts at the sequence edges. Second, while the LSWT learns task-specific filters, these weights remain static during inference. In addition, the model’s ability to capture local semantics is sensitive to the initial patch size  $P$ . If  $P$  is not well-aligned with the underlying periodicity of the data, the Neighboring Mixer Block may struggle to extract coherent patterns, necessitating careful hyperparameter tuning.

Future work will focus on developing a flexible, length-adaptive patching mechanism to mitigate padding artifacts and exploring dynamic filter adaptation strategies to better handle non-stationary concept drift. We also plan to investigate multi-resolution alignment techniques to reduce sensitivity to patch size selection.

## Impact Statement

This paper presents work whose goal is to advance the field of machine learning in the domain of long-term time series forecasting. Our proposed **NPMixer** architecture improves the accuracy of modeling complex temporal dynamics, which has potential positive societal impacts in areas such as energy grid optimization, weather forecasting, and logistics planning. For instance, improved forecasting accuracy in renewable energy sectors can lead to more efficient power scheduling and reduced carbon footprints.

However, we acknowledge that time series forecasting models rely heavily on historical data. If the training data contains biases or reflects historical inequities (e.g., in economic or resource allocation data), the model may inadvertently keep these patterns in its future predictions. Additionally, there is a risk of over-reliance on algorithmic outputs in critical decision-making processes. We encourage practitioners to rigorously validate model outputs against domain expertise, particularly when applied to sensitive or high-stakes environments.

## References

- Akiba, T., Sano, S., Yanase, T., Ohta, T., and Koyama, M. Optuna: A next-generation hyperparameter optimization framework, 2019.
- Box, G. E., Jenkins, G. M., Reinsel, G. C., and Ljung, G. M. *Time series analysis: forecasting and control*. John Wiley & Sons, 2015.
- Cai, W., Liang, Y., Liu, X., Feng, J., and Wu, Y. Msgnet: Learning multi-scale inter-series correlations for multivariate time series forecasting. In *AAAI*, 2024.
- California Department of Transportation (Caltrans). Performance measurement system (PeMS). <https://pems.dot.ca.gov/>, 2024. Accessed: 2024-05-20.
- Chen, H., Luong, V., Mukherjee, L., and Singh, V. SimpleTM: A simple baseline for multivariate time series forecasting. In *ICLR*, 2025.
- Chen, S.-A., Li, C.-L., Arik, S. O., Yoder, N. C., and Pfister, T. TSMixer: An all-MLP architecture for time series forecasting. *TMLR*, 2023.
- Dosovitskiy, A., Beyer, L., Kolesnikov, A., Weissenborn, D., Zhai, X., Unterthiner, T., Dehghani, M., Minderer, M., Heigold, G., Gelly, S., Uszkoreit, J., and Housley, N. An image is worth 16x16 words: Transformers for image recognition at scale. In *ICLR*, 2021.
- Ekambaram, V., Jati, A., Nguyen, N., Sinthong, P., and Kalagnanam, J. Tsmixer: Lightweight mlp-mixer model for multivariate time series forecasting. In *ACM SIGKDD*, 2023.
- Gontijo-Lopes, R., Dauphin, Y., and Cubuk, E. D. No one representation to rule them all: Overlapping features of training methods. *arXiv preprint arXiv:2110.12899*, 2021.
- Heil, C. E. and Walnut, D. F. Continuous and discrete wavelet transforms. *SIAM review*, 31(4):628–666, 1989.
- Huang, Q., Shen, L., Zhang, R., Ding, S., Wang, B., Zhou, Z., and Wang, Y. Crossggn: Confronting noisy multivariate time series via cross interaction refinement. *Advances in Neural Information Processing Systems*, 36: 46885–46902, 2023.
- Kim, T., Kim, J., Tae, Y., Park, C., Choi, J.-H., and Choo, J. Reversible instance normalization for accurate time-series forecasting against distribution shift. In *International Conference on Learning Representations*, 2022.
- Liu, Y., Hu, T., Zhang, H., Wu, H., Wang, S., Ma, L., and Long, M. itransformer: Inverted transformers are effective for time series forecasting. In *ICLR*, 2024.
- Liu, Z., Lin, Y., Cao, Y., Hu, H., Wei, Y., Zhang, Z., Lin, S., and Guo, B. Swin transformer: Hierarchical vision transformer using shifted windows. In *IEEE/CVF*, 2021.
- Max Planck Institute for Biogeochemistry. Jena climate dataset. <https://www.bgc-jena.mpg.de/wetter/>, 2024. Accessed: 2024-05-20.
- Michau, G., Frusque, G., and Fink, O. Fully learnable deep wavelet transform for unsupervised monitoring of high-frequency time series. *Proceedings of the National Academy of Sciences*, 119(8):e2106598119, 2022. doi: 10.1073/pnas.2106598119.
- Nason, G. P. and Silverman, B. W. *The Stationary Wavelet Transform and some Statistical Applications*, pp. 281–299. Springer New York, New York, NY, 1995. ISBN 978-1-4612-2544-7.
- Nie, Y., Nguyen, N. H., Sinthong, P., and Kalagnanam, J. A time series is worth 64 words: Long-term forecasting with transformers. In *ICLR*, 2023.
- Qiu, X., Hu, J., Zhou, L., Wu, X., Du, J., Zhang, B., Guo, C., Zhou, A., Jensen, C. S., Sheng, Z., et al. Tfb: Towards comprehensive and fair benchmarking of time series forecasting methods. *arXiv preprint arXiv:2403.20150*, 2024.
- Trindade, A. ElectricityLoadDiagrams20112014. UCI Machine Learning Repository, 2015. DOI: <https://doi.org/10.24432/C58C86>.
- Vaswani, A., Shazeer, N., Parmar, N., Uszkoreit, J., Jones, L., Gomez, A. N., Kaiser, L., and Polosukhin, I. Attention is all you need. *NeurIPS*, 2017.
- Wang, H., Peng, J., Huang, F., Wang, J., Chen, J., and Xiao, Y. Micn: Multi-scale local and global context modeling for long-term series forecasting. In *The eleventh international conference on learning representations*, 2023.
- Wang, S., Wu, H., Shi, X., Hu, T., Luo, H., Ma, L., Zhang, J. Y., and ZHOU, J. Timemixer: Decomposable multi-scale mixing for time series forecasting. In *ICLR*, 2024a.

- Wang, Y., Wu, H., Dong, J., Qin, G., Zhang, H., Liu, Y., Qiu, Y., Wang, J., and Long, M. Timexer: Empowering transformers for time series forecasting with exogenous variables. *Advances in Neural Information Processing Systems*, 37:469–498, 2024b.
- Wu, H., Xu, J., Wang, J., and Long, M. Autoformer: Decomposition transformers with auto-correlation for long-term series forecasting. *NeurIPS*, 2021.
- Wu, H., Hu, T., Liu, Y., Zhou, H., Wang, J., and Long, M. Timesnet: Temporal 2d-variation modeling for general time series analysis, 2023.
- Yang, F., Li, X., Wang, M., Zang, H., Pang, W., and Wang, M. Waveform: Graph enhanced wavelet learning for long sequence forecasting of multivariate time series. *AAAI*, Jun. 2023.
- Yi, K., Zhang, Q., Fan, W., Wang, S., Wang, P., He, H., An, N., Lian, D., Cao, L., and Niu, Z. Frequency-domain mlps are more effective learners in time series forecasting. *NeurIPS*, 2023.
- Zeng, A., Chen, M., Zhang, L., and Xu, Q. Are transformers effective for time series forecasting? In *AAAI*, 2023.
- Zhang, Y. and Yan, J. Crossformer: Transformer utilizing cross-dimension dependency for multivariate time series forecasting. In *ICLR*, 2023.
- Zhou, H., Zhang, S., Peng, J., Zhang, S., Li, J., Xiong, H., and Zhang, W. Informer: Beyond efficient transformer for long sequence time-series forecasting. In *AAAI*, 2021.
- Zhou, T., Ma, Z., Wen, Q., Wang, X., Sun, L., and Jin, R. Fedformer: Frequency enhanced decomposed transformer for long-term series forecasting. In *International conference on machine learning*. PMLR, 2022.

## A. Experimental Settings

### A.1. Datasets

To evaluate the robustness of NPMixer, we conduct extensive experiments on seven long-term time series forecasting benchmark datasets. These datasets encompass diverse domains including energy, weather, and transportation, with varying temporal resolutions and channel dimensions.

- **ETT (Electricity Transformer Temperature):** This dataset includes seven electricity-related factors. It is divided into four subsets: ETTh1 and ETTh2 are sampled at 1-hour intervals, while ETTm1 and ETTm2 are sampled at 15-minute intervals (Zhou et al., 2021).
- **ECL (Electricity Consumption Load):** This dataset tracks the hourly power usage of 321 distinct clients, providing a high-dimensional challenge for multivariate modeling (Wu et al., 2021).
- **Weather:** Comprising 21 meteorological indicators (e.g., humidity, temperature), these data points were recorded every 10 minutes throughout 2020 at the Max Planck Institute for Biogeochemistry (Wu et al., 2021).
- **Traffic:** This collection consists of hourly road occupancy rates recorded by 862 sensors located across San Francisco Bay Area freeways over a two-year period (Wu et al., 2021).

The detailed statistics for each dataset, including the number of channels ( $C$ ), total time steps ( $T$ ), and the specific train/validation/test splits, are summarized in Table 4. Following standard evaluation protocols, the look-back window size ( $L$ ) is fixed at 96 for general performance comparison, while we evaluate performance across prediction horizons ( $H$ ) of  $\{96, 192, 336, 720\}$ . Additionally, to investigate the impact of temporal context, we conduct look-back window tuning where  $L$  is varied within the set  $\{96, 192, 336, 512\}$ .

Table 4. Summary of dataset statistics and experimental configurations. The input length  $L$  is fixed at 96 for standard comparisons and tuned within  $\{96, 192, 336, 512\}$  for look-back window analysis.

Dataset	Statistics		Dataset Split	Size of Input & Output	
	$C$	$T$		$L$	$H$
ETTh1 (Zhou et al., 2021)	7	17,420	(8,545, 2,881, 2,881)	96 / {96, 192, 336, 512}	{96, 192, 336, 720}
ETTh2 (Zhou et al., 2021)	7	17,420	(8,545, 2,881, 2,881)		
ETTh1 (Zhou et al., 2021)	7	69,680	(34,465, 11,521, 11,521)		
ETTh2 (Zhou et al., 2021)	7	69,680	(34,465, 11,521, 11,521)		
Weather (Wu et al., 2021)	21	52,696	(36,792, 5,271, 10,540)		
ECL (Wu et al., 2021)	321	26,304	(18,317, 2,633, 5,261)		
Traffic (Wu et al., 2021)	862	17,544	(12,185, 1,756, 3,508)		

### A.2. Hyperparameter Optimization

#### A.2.1. HYPERPARAMETER SPACE

We employ the Optuna framework (Akiba et al., 2019) for automated hyperparameter optimization. We utilize the Tree-structured Parzen Estimator (TPE) sampler to ensure reproducibility during the search process. For each prediction horizon  $H \in \{96, 192, 336, 720\}$ , we conduct a hyperparameter search aimed at minimizing the validation Mean Squared Error (MSE).

The comprehensive search space, encompassing architectural parameters, wavelet configurations, and training dynamics, is detailed in Table 5.

### A.3. Optimal Hyperparameter Configurations

The following table summarizes the best-performing hyperparameter configurations identified via the Optuna optimization process. These parameters were utilized to produce the main experimental results for  $L = 96$ .

Table 5. Hyperparameter search space for Optuna optimization.

Hyperparameter	Search Space / Values
Learning Rate	Float $\in [10^{-4}, 10^{-2}]$ (Log-scale)
$d_{model}$	{32, 64, 128, 256, 512, 1024}
$d_{ff}$	{32, 64, 128, 256, 512, 1024, 2048}
Encoder Layers ( $e_{layers}$ )	Integer $\in [1, 5]$
Dropout	Float $\in [0.2, 0.8]$ (Log-scale)
Wavelet Levels ( $J$ )	Integer $\in [1, 5]$
Wavelet Type	{db1, db2, db5, sym3, sym4, sym5, coif5, bior3.1}
Patch Size	{4, 8, 12, 16, 24, 32, 48}

Table 6. Best hyperparameter configurations for ETT, ECL, Weather, and Traffic across horizons  $H \in \{96, 192, 336, 720\}$ .

Dataset	$H$	LR	$d_{model}$	$d_{ff}$	$e_{layers}$	Drop	$J$	Wavelet	Patch	Batch
ETTh1	96	1.51e-3	64	1024	1	0.28	1	db2	24	256
	192	8.08e-3	1024	256	4	0.77	4	db1	16	64
	336	4.64e-3	1024	1024	5	0.81	4	db1	4	64
	720	1.70e-3	128	512	4	0.58	1	sym4	24	256
ETTh2	96	3.47e-3	512	1024	5	0.73	1	db1	32	64
	192	4.62e-3	64	128	3	0.55	3	db1	48	64
	336	1.67e-3	64	128	3	0.17	5	db2	4	256
	720	3.66e-4	256	128	1	0.24	4	db2	24	256
ETTh1	96	3.75e-3	256	128	5	0.35	1	db2	12	64
	192	5.07e-3	512	32	2	0.69	4	db3	16	64
	336	2.03e-3	512	256	3	0.76	1	db5	8	64
	720	5.64e-3	128	2048	3	0.47	3	db5	48	64
ETTh2	96	5.25e-3	64	128	1	0.55	2	bior3.1	12	64
	192	5.07e-3	512	32	2	0.69	4	db2	16	64
	336	1.22e-3	128	256	2	0.88	5	db2	24	64
	720	3.05e-3	64	2048	4	0.80	2	db2	32	64
ECL	96	3.12e-3	128	128	1	0.31	5	sym4	16	32
	192	1.23e-3	256	512	2	0.16	4	db1	12	32
	336	1.17e-3	128	512	4	0.11	4	db1	4	32
	720	3.12e-3	128	128	1	0.31	5	db1	16	32
Weather	96	1.20e-3	32	64	1	0.44	4	db4	4	32
	192	1.61e-3	32	512	3	0.17	2	db4	4	32
	336	5.24e-4	32	64	3	0.64	3	db4	4	32
	720	2.03e-3	128	128	1	0.11	5	db4	4	32
Traffic	96	2.99e-4	512	2048	3	0.44	3	db1	48	8
	192	4.49e-4	512	1024	2	0.46	4	db1	48	8
	336	8.23e-4	256	1024	2	0.45	4	db1	8	8
	720	4.12e-4	256	2048	4	0.41	2	db1	32	8

The following table presents the optimal hyperparameter configurations identified during our look-back window search. Through extensive tuning across the candidate set  $L \in \{96, 192, 336, 512\}$ , the model consistently outperforms the other models with a look-back window of  $L = 512$  across all benchmark datasets. This indicates that a larger temporal context is highly beneficial for the NPMixer architecture to capture the underlying long-range dependencies effectively.

Table 7. Best hyperparameter configurations for ETT, ECL, Weather, and Traffic for look-back window tuned experiments.

Dataset	$L$	$H$	LR	$d_{model}$	$d_{ff}$	$e_{layers}$	Drop	$J$	Wavelet	Patch	Batch
ETTh1	512	96	1.10e-3	256	2048	2	0.88	2	db1	24	64
ETTh1	512	192	4.94e-4	32	512	1	0.35	1	db2	96	64
ETTh1	512	336	2.11e-4	64	512	2	0.38	2	db3	128	64
ETTh1	512	720	1.96e-4	64	1024	3	0.79	3	db1	12	64
ETTh2	512	96	2.19e-4	32	64	4	0.46	5	bior3.1	16	256
ETTh2	512	192	8.37e-4	32	64	5	0.79	4	db2	96	256
ETTh2	512	336	3.19e-4	32	32	5	0.66	1	db1	16	256
ETTh2	512	720	4.89e-4	64	128	1	0.57	4	db1	96	256
ETTh1	512	96	4.17e-3	32	512	3	0.54	3	db3	128	64
ETTh1	512	192	1.61e-4	32	512	1	0.36	1	db3	256	64
ETTh1	512	336	4.58e-3	128	2048	5	0.49	3	db2	256	64
ETTh1	512	720	2.78e-4	1024	1024	5	0.48	3	db5	256	64
ETTh2	512	96	4.21e-4	32	128	4	0.38	4	bior3.1	96	64
ETTh2	512	192	9.08e-3	64	128	4	0.58	2	bior3.1	256	64
ETTh2	512	336	4.47e-3	64	512	2	0.58	3	db3	128	64
ETTh2	512	720	3.31e-3	64	256	5	0.72	3	db2	128	64
ECL	512	96	6.00e-3	64	2048	2	0.62	4	db1	24	16
ECL	512	192	2.41e-3	256	2048	3	0.71	4	db2	48	16
ECL	512	336	3.02e-3	512	2048	5	0.48	2	db2	256	16
ECL	512	720	1.83e-4	512	256	3	0.29	2	sym3	256	16
Weather	512	96	1.50e-4	32	1024	1	0.55	2	db3	32	32
Weather	512	192	1.33e-4	32	64	2	0.59	4	db3	128	32
Weather	512	336	2.18e-4	32	128	2	0.31	1	db2	256	32
Weather	512	720	1.03e-4	32	64	3	0.78	4	db2	32	32
Traffic	512	96	5.36e-4	128	1024	5	0.35	3	db1	128	8
Traffic	512	192	4.69e-4	128	2048	4	0.48	2	bior3.1	96	8
Traffic	512	336	4.09e-3	512	512	4	0.32	1	db1	32	8
Traffic	512	720	4.23e-3	256	64	5	0.25	2	bior3.1	256	8

## B. Extended Experimental Results

In this section, we provide a comprehensive analysis of the performance and robustness of the proposed NPMixer model. We first present the stability results across multiple random seeds to demonstrate consistent performance. Furthermore, we include a detailed evaluation of look-back window tuning and the ablation study to validate the contribution of each model component.

Table 8. Standard deviation ( $\pm$ std) of MSE and MAE across three random seeds over different prediction horizons with a fixed look-back window ( $L = 96$ ).

Dataset	Horizon	NPMixer (Ours)	
		MSE	MAE
ETTm1	96	$\pm 0.002$	$\pm 0.001$
	192	$\pm 0.000$	$\pm 0.000$
	336	$\pm 0.000$	$\pm 0.000$
	720	$\pm 0.001$	$\pm 0.000$
ETTm2	96	$\pm 0.001$	$\pm 0.001$
	192	$\pm 0.000$	$\pm 0.001$
	336	$\pm 0.000$	$\pm 0.000$
	720	$\pm 0.000$	$\pm 0.000$
ETTh1	96	$\pm 0.002$	$\pm 0.001$
	192	$\pm 0.002$	$\pm 0.000$
	336	$\pm 0.002$	$\pm 0.003$
	720	$\pm 0.000$	$\pm 0.000$
ETTh2	96	$\pm 0.002$	$\pm 0.001$
	192	$\pm 0.000$	$\pm 0.000$
	336	$\pm 0.006$	$\pm 0.002$
	720	$\pm 0.001$	$\pm 0.001$
Electricity	96	$\pm 0.000$	$\pm 0.000$
	192	$\pm 0.000$	$\pm 0.000$
	336	$\pm 0.000$	$\pm 0.000$
	720	$\pm 0.003$	$\pm 0.002$
Traffic	96	$\pm 0.000$	$\pm 0.001$
	192	$\pm 0.001$	$\pm 0.000$
	336	$\pm 0.001$	$\pm 0.000$
	720	$\pm 0.000$	$\pm 0.000$
Weather	96	$\pm 0.001$	$\pm 0.000$
	192	$\pm 0.001$	$\pm 0.000$
	336	$\pm 0.000$	$\pm 0.001$
	720	$\pm 0.000$	$\pm 0.000$

Table 9. Ablation study of NPMixer: Average MSE and MAE across three random seeds over different prediction horizons.

Dataset	Horizon	NPMixer		w/o SWT		w/o Learnable SWT		w/o Neighboring Mixer		w/o Channel-Mixing Encoder	
		MSE	MAE	MSE	MAE	MSE	MAE	MSE	MAE	MSE	MAE
ETTh1	96	<u>0.306</u>	<b>0.348</b>	0.310	0.351	<b>0.305</b>	<u>0.349</u>	0.314	0.359	0.310	0.351
	192	<b>0.344</b>	<b>0.373</b>	0.350	<b>0.373</b>	<u>0.347</u>	0.375	0.361	0.386	0.359	0.381
	336	<b>0.370</b>	<b>0.395</b>	0.377	<u>0.396</u>	<u>0.371</u>	<b>0.395</b>	0.402	0.411	0.375	0.397
	720	<b>0.431</b>	<b>0.429</b>	0.448	0.433	<u>0.436</u>	<u>0.431</u>	0.467	0.454	0.442	0.435
ETTh2	96	<b>0.166</b>	<b>0.250</b>	<u>0.170</u>	<u>0.254</u>	0.171	0.255	0.176	0.260	0.172	0.256
	192	<b>0.234</b>	<b>0.296</b>	<u>0.236</u>	<b>0.296</b>	0.238	0.301	0.242	0.302	0.245	0.306
	336	<b>0.291</b>	<b>0.332</b>	0.298	0.337	0.292	<u>0.333</u>	0.298	0.339	<b>0.291</b>	<b>0.332</b>
	720	<b>0.390</b>	<b>0.390</b>	0.394	<u>0.392</u>	0.395	0.393	0.400	0.399	<u>0.393</u>	0.392
ETTh1	96	<b>0.361</b>	<u>0.392</u>	0.371	<u>0.392</u>	<u>0.364</u>	<b>0.391</b>	0.390	0.408	0.371	0.398
	192	<b>0.419</b>	0.429	<b>0.419</b>	<b>0.423</b>	0.439	0.433	0.446	0.443	<u>0.434</u>	<u>0.427</u>
	336	<b>0.455</b>	0.451	<u>0.468</u>	<b>0.449</b>	0.481	0.456	0.485	0.461	0.477	<u>0.450</u>
	720	<b>0.458</b>	<b>0.461</b>	<b>0.458</b>	<b>0.461</b>	<u>0.491</u>	0.486	0.500	0.477	0.503	0.482
ETTh2	96	<b>0.280</b>	<b>0.337</b>	0.290	0.340	<u>0.284</u>	<u>0.338</u>	0.292	0.348	<b>0.280</b>	<b>0.337</b>
	192	<b>0.354</b>	<b>0.383</b>	0.367	0.389	<u>0.355</u>	<u>0.383</u>	0.389	0.401	0.360	0.388
	336	<b>0.408</b>	<b>0.424</b>	0.417	0.428	<u>0.412</u>	<u>0.424</u>	0.426	0.434	0.416	0.428
	720	<b>0.413</b>	<b>0.435</b>	0.428	0.445	<u>0.425</u>	0.443	0.426	<u>0.442</u>	0.427	0.444
Electricity	96	<b>0.138</b>	<b>0.235</b>	<u>0.146</u>	<u>0.240</u>	0.146	0.241	0.158	0.258	0.155	0.247
	192	<b>0.157</b>	<u>0.253</u>	0.159	<u>0.253</u>	<u>0.157</u>	<b>0.252</b>	0.180	0.280	0.167	0.258
	336	<b>0.172</b>	<b>0.267</b>	<u>0.177</u>	<u>0.269</u>	<u>0.177</u>	0.272	0.193	0.294	0.185	0.277
	720	<b>0.205</b>	<b>0.299</b>	<u>0.207</u>	<u>0.300</u>	<u>0.207</u>	0.301	0.223	0.322	0.227	0.317
Traffic	96	<b>0.404</b>	<b>0.279</b>	<b>0.404</b>	<b>0.279</b>	0.410	<u>0.281</u>	0.509	0.351	0.498	0.326
	192	<b>0.433</b>	<b>0.293</b>	<b>0.433</b>	<b>0.293</b>	<u>0.440</u>	<u>0.299</u>	0.508	0.353	0.495	0.325
	336	<b>0.449</b>	<b>0.301</b>	<b>0.449</b>	<b>0.301</b>	<u>0.462</u>	<u>0.305</u>	0.516	0.350	0.512	0.322
	720	<b>0.484</b>	<b>0.317</b>	<b>0.484</b>	0.318	0.486	<b>0.317</b>	0.557	0.371	0.567	0.363
Weather	96	<b>0.154</b>	<b>0.202</b>	0.167	0.211	0.162	0.206	<u>0.155</u>	<u>0.204</u>	0.160	0.207
	192	<b>0.204</b>	<b>0.248</b>	0.210	0.250	0.208	0.249	<b>0.204</b>	<u>0.249</u>	0.206	<u>0.249</u>
	336	<b>0.261</b>	<b>0.287</b>	0.277	0.297	0.268	0.291	<b>0.258</b>	<u>0.287</u>	0.262	0.290
	720	<b>0.340</b>	<b>0.338</b>	0.344	0.343	0.343	<u>0.342</u>	0.352	0.353	<u>0.342</u>	0.343

Table 10. Full results of look-back window tuned results.

Models	NPMixer (Ours)		TimeMixer 2024		PatchTST 2023		TSMixer 2023		TimesNet 2023		Crossformer 2023		FiLM 2022a		DLinear 2023		
Metric	MSE	MAE	MSE	MAE	MSE	MAE	MSE	MAE	MSE	MAE	MSE	MAE	MSE	MAE	MSE	MAE	
ETTh1	96	0.362	0.391	<b>0.361</b>	<b>0.390</b>	0.370	0.400	<b>0.361</b>	0.392	0.384	0.402	0.418	0.438	0.422	0.432	0.375	0.399
	192	<b>0.400</b>	0.417	0.409	<b>0.414</b>	0.413	0.429	<u>0.404</u>	0.418	0.436	0.429	0.539	0.517	0.462	0.458	0.405	<u>0.416</u>
	336	0.423	0.434	0.430	<b>0.429</b>	<u>0.422</u>	0.440	<b>0.420</b>	<u>0.431</u>	0.491	0.469	0.709	0.638	0.501	0.483	0.439	<u>0.443</u>
	720	0.455	<u>0.464</u>	<b>0.445</b>	<b>0.460</b>	<u>0.447</u>	0.468	0.463	0.472	0.521	0.500	0.733	0.636	0.544	0.526	0.472	0.490
	Avg	<b>0.410</b>	<u>0.426</u>	<u>0.411</u>	<b>0.423</b>	0.413	0.434	0.412	0.428	0.458	0.450	0.600	0.557	0.482	0.475	0.423	0.437
ETTh2	96	<b>0.267</b>	<u>0.336</u>	<u>0.271</u>	<b>0.330</b>	0.274	0.337	0.274	0.341	0.340	0.374	0.425	0.463	0.323	0.370	0.289	0.353
	192	<u>0.320</u>	<b>0.377</b>	<b>0.317</b>	0.402	0.341	<u>0.382</u>	0.339	0.385	0.402	0.414	0.473	0.500	0.391	0.415	0.383	0.418
	336	0.358	0.405	<u>0.332</u>	<u>0.396</u>	<b>0.329</b>	<b>0.384</b>	0.361	0.406	0.452	0.452	0.581	0.562	0.415	0.440	0.448	0.465
	720	0.398	0.436	<b>0.342</b>	<b>0.408</b>	<u>0.379</u>	<u>0.422</u>	0.445	0.470	0.462	0.468	0.775	0.665	0.441	0.459	0.605	0.551
	Avg	0.336	0.388	<b>0.316</b>	<u>0.384</u>	<u>0.331</u>	<b>0.381</b>	0.355	0.401	0.414	0.427	0.564	0.548	0.393	0.421	0.431	0.447
ETTm1	96	0.322	0.365	<u>0.291</u>	<u>0.340</u>	0.293	0.346	<b>0.285</b>	<b>0.339</b>	0.338	0.375	0.361	0.403	0.302	0.345	0.299	0.343
	192	<b>0.314</b>	<b>0.356</b>	<u>0.327</u>	<u>0.365</u>	0.333	0.370	<u>0.327</u>	<u>0.365</u>	0.374	0.387	0.387	0.422	0.338	0.368	0.335	<u>0.365</u>
	336	<b>0.350</b>	<b>0.379</b>	0.360	<u>0.381</u>	0.369	0.392	<u>0.356</u>	<u>0.382</u>	0.410	0.411	0.605	0.572	0.373	0.388	0.369	0.386
	720	<b>0.386</b>	<b>0.408</b>	<u>0.415</u>	0.417	0.416	0.420	0.419	<u>0.414</u>	0.478	0.450	0.703	0.645	0.420	0.420	0.425	0.421
	Avg	<b>0.343</b>	0.377	0.348	<b>0.375</b>	0.353	0.382	<u>0.347</u>	<b>0.375</b>	0.400	0.406	0.514	0.510	0.358	0.380	0.357	0.379
ETTm2	96	<b>0.162</b>	<b>0.252</b>	0.164	0.254	0.166	0.256	<u>0.163</u>	<b>0.252</b>	0.187	0.267	0.275	0.358	0.165	0.256	0.167	0.260
	192	<b>0.214</b>	<b>0.287</b>	0.223	0.295	0.223	0.296	<u>0.216</u>	<u>0.290</u>	0.249	0.309	0.345	0.400	0.222	0.296	0.224	0.303
	336	<u>0.274</u>	0.330	0.279	0.330	<u>0.274</u>	<u>0.329</u>	<b>0.268</b>	<b>0.324</b>	0.321	0.351	0.657	0.528	0.277	0.333	0.281	0.342
	720	<b>0.358</b>	<b>0.381</b>	<u>0.359</u>	<u>0.383</u>	<u>0.362</u>	<u>0.385</u>	0.420	0.422	0.408	0.403	1.208	0.753	0.371	0.389	0.397	0.421
	Avg	<b>0.252</b>	<b>0.312</b>	<u>0.256</u>	<u>0.315</u>	<u>0.256</u>	0.317	0.267	0.322	0.291	0.333	0.621	0.510	0.259	0.319	0.267	0.332
Weather	96	<b>0.140</b>	<b>0.189</b>	0.147	<u>0.197</u>	0.149	0.198	<u>0.145</u>	0.198	0.172	0.220	0.232	0.302	0.199	0.262	0.176	0.237
	192	<b>0.182</b>	<b>0.232</b>	<u>0.189</u>	<u>0.239</u>	0.194	0.241	0.191	0.242	0.219	0.261	0.371	0.410	0.228	0.288	0.220	0.282
	336	<b>0.237</b>	<b>0.275</b>	<u>0.241</u>	<u>0.280</u>	0.245	0.282	0.242	<u>0.280</u>	0.280	0.306	0.495	0.515	0.267	0.323	0.265	0.319
	720	<b>0.304</b>	<b>0.322</b>	<u>0.310</u>	<u>0.330</u>	0.314	0.334	0.320	<u>0.336</u>	0.365	0.359	0.526	0.542	0.319	0.361	0.323	0.362
	Avg	<b>0.216</b>	<b>0.254</b>	<u>0.222</u>	<u>0.262</u>	0.226	0.264	0.225	0.264	0.259	0.287	0.406	0.442	0.253	0.309	0.246	0.300
Electricity	96	<b>0.128</b>	<b>0.196</b>	<u>0.129</u>	0.224	<u>0.129</u>	<u>0.222</u>	0.131	0.229	0.168	0.272	0.150	0.251	0.154	0.267	0.140	0.237
	192	0.151	0.245	<b>0.140</b>	<b>0.220</b>	<u>0.147</u>	<u>0.240</u>	0.151	0.246	0.184	0.289	0.161	0.260	0.164	0.258	0.153	0.249
	336	0.171	0.265	<b>0.161</b>	<b>0.255</b>	0.163	<u>0.259</u>	<b>0.161</b>	0.261	0.198	0.300	0.182	0.281	0.188	0.283	0.169	0.267
	720	<b>0.173</b>	<b>0.253</b>	<u>0.194</u>	<u>0.287</u>	0.197	0.290	0.197	0.293	0.220	0.320	0.251	0.339	0.236	0.332	0.203	0.301
	Avg	<b>0.156</b>	<b>0.240</b>	<u>0.156</u>	<u>0.246</u>	0.159	0.253	0.160	0.257	0.192	0.295	0.186	0.283	0.186	0.285	0.166	0.264
Traffic	96	<b>0.358</b>	0.255	<u>0.360</u>	<b>0.249</b>	<u>0.360</u>	<b>0.249</b>	0.376	0.264	0.593	0.321	0.514	0.267	0.416	0.294	0.410	0.282
	192	0.384	0.268	<b>0.375</b>	<b>0.250</b>	<u>0.379</u>	0.256	0.397	0.277	0.617	0.336	0.549	<u>0.252</u>	0.408	0.288	0.423	0.287
	336	0.393	<u>0.266</u>	<b>0.385</b>	0.270	<u>0.392</u>	<b>0.264</b>	0.413	0.290	0.629	0.336	0.530	0.300	0.425	0.298	0.436	0.296
	720	<b>0.429</b>	0.289	0.430	<b>0.281</b>	0.432	<u>0.286</u>	0.444	0.306	0.640	0.350	0.573	0.313	0.520	0.353	0.466	0.315
	Avg	<u>0.391</u>	0.270	<b>0.387</b>	<b>0.262</b>	<u>0.391</u>	<u>0.264</u>	0.408	0.284	0.620	0.336	0.542	0.283	0.442	0.308	0.434	0.295
1st Count:	21	16	11	14	1	4	5	4	0	0	0	0	0	0	0	0	0

### C. An Example of the Process of Neighboring Mixer Block

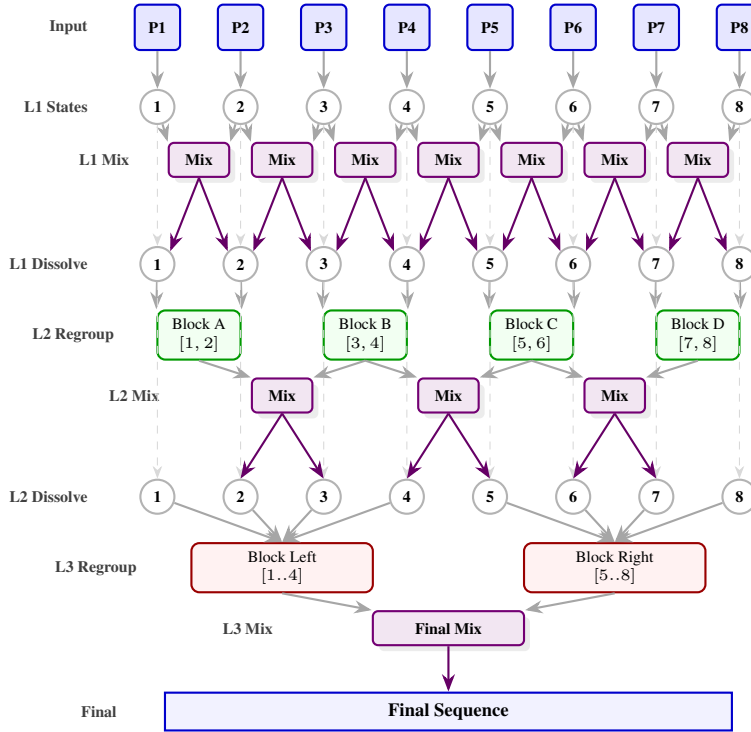


Figure 3. Hierarchical patch mixing process.

**An 8-Patch Case** To illustrate the hierarchical mixing mechanism, we consider a sequence of  $N = 8$  patches as shown in Figure 3. The process begins with locally processed patches and expands exponentially into global mixing through three distinct stages ( $K = 3$ ), alternating between grouping states into blocks and dissolving them back into individual patch representations:

- **Step 1: Intra-Patch Processing.** Before any interaction occurs, each of the 8 patches  $P_i$  is independently processed by a shared S-MLP. This results in the initial **Level 1 States** (1, 2, ..., 8), which contain rich but isolated temporal features.
- **Step 2: Level 1 Mixing (Pairwise).** The patches undergo the first relation operation. The model mixes adjacent states via 7 overlapping pairs, e.g., 1–2 and 2–3. After mixing, the relational information is **dissolved** back into the individual patch streams, producing the refined **Level 2 States**.
- **Step 3: Level 2 Mixing (Block Size 2).** The refined states are explicitly **regrouped** into 4 non-overlapping blocks: *Block A* [1, 2], *Block B* [3, 4], *Block C* [5, 6], and *Block D* [7, 8]. The mixer then operates on overlapping pairs of these blocks, e.g., mixing *Block A* with *Block B*. Following this interaction, the blocks are once again **dissolved**, distributing the expanded contextual information back to the individual patches to form the **Level 3 States**.
- **Step 4: Level 3 Mixing (Block Size 4).** In the final stage, the states are **regrouped** into two large blocks: *Block Left* with patches 1–4 and *Block Right* with patches 5–8. A final mixing operation bridges these two halves. The result is dissolved into the final sequence, ensuring that every patch has effectively exchanged information with the entire sequence relative to its position.

## D. Efficiency Analysis

Table 11. Comparison of NPMixer (Ours) and SimpleTM across Weather and ETTm1 datasets ( $L = 96, T = 96$ , batch size = 64 for ETTm1, 32 for Weather).

Dataset	Model	MSE ↓	Total Params	GFLOPs	Speed (s/iter) ↓
Weather	NPMixer (Ours)	<b>0.154</b>	126,111	0.1325	<b>0.1620</b>
	SimpleTM	0.162	<b>14,880</b>	<b>0.0099</b>	0.2424
ETTM1	NPMixer (Ours)	<b>0.306</b>	2,365,686	0.9802	<b>0.1518</b>
	SimpleTM	0.321	<b>1,700,576</b>	<b>0.7611</b>	0.4210

The efficiency analysis presented in Table 11 reveals a significant advantage of NPMixer in practical deployment scenarios. While NPMixer occupies a larger footprint in terms of total parameters and computational GFLOPs compared to the lightweight SimpleTM, it consistently outperforms SimpleTM in both predictive accuracy and execution speed.

Specifically, on the ETTm1 dataset, although NPMixer has approximately 39% more parameters and 28% higher GFLOPs than SimpleTM, it records a training speed that is nearly  $2.7\times$  faster (0.1518 vs. 0.4210 s/iter). This can be attributed to the structured, non-overlapping patch processing and hierarchical MLP blocks in our model, which are highly optimized for parallel execution on modern GPUs. Furthermore, the NPMixer architecture achieves a better balance between complexity and performance, yielding a substantial improvement in MSE (0.306 vs. 0.321). These results underscore that NPMixer is not only more accurate but also more computationally efficient for high-throughput time series forecasting tasks.